

## SLOW CHANGES IN CURRENTS THROUGH SODIUM CHANNELS IN FROG MUSCLE MEMBRANE

BY W. ALMERS, P. R. STANFIELD\* AND W. STÜHMER

*From the Department of Physiology and Biophysics, SJ-40, University of Washington, Seattle, WA 98195, U.S.A.*

(Received 26 October 1982)

### SUMMARY

1. We used a patch clamp to measure Na currents across 10–15  $\mu\text{m}$  diameter circular patches of frog and rat skeletal muscle membrane. We tested for electrophoretic mobility of Na channels, by applying steady lateral fields (of the order of 10 mV  $\mu\text{m}^{-1}$ ) across the wall of the patch pipette.

2. Application of steady negative potentials to the inside of the pipette resulted in a fall in the number of functional Na channels in the patch. This fall took several minutes to complete and was reversible. It was assayed by applying suitable depolarizations at approximately 11 sec intervals.

3. When a steady lateral field was applied in the absence of changes in membrane potential of the patch, the loss of Na current was virtually abolished. Thus it was not due to electrophoretic movement of channels, but instead to depolarization of the sarcolemma. Evidently, a very slow inactivation of Na conductance operates in skeletal muscle.

4. In frog muscle, the rate constants for loss and recovery of Na current were about 0.1  $\text{min}^{-1}$  (17 °C) at resting potential. Rate constants were higher at more positive and at more negative membrane potentials. Current amplitude was reduced to 0.5 at about  $-76$  mV.

5. Roughly similar results were found in rat omohyoid muscle. A further inactivation mechanism, whose rate was intermediate between conventional fast inactivation and the very slow process described here, was present also in both rat and frog muscle.

6. In frog muscle, lateral fields do not alter the potential dependence of fast inactivation. Either the surface charge due to membrane lipids does not influence inactivation or the lipids immediately surrounding the Na channel are restricted in their mobility.

### INTRODUCTION

This paper investigates the possibility that Na channels of frog muscle fibres may be moved laterally in the sarcolemma by an electrical field applied across the rim of a glass micropipette pressed against the surface.

\* Present address: Department of Physiology, University of Leicester, University Road, Leicester, LE1 7RH.

As Poo (1981) has recently reviewed, a number of membrane constituents in embryonic *Xenopus* muscle may be moved by quite small lateral fields (Poo, Poo & Lam, 1978; Orida & Poo, 1978). The movement is believed to result either by direct action on the intrinsic charge of the moving membrane constituent or as a consequence of electro-osmosis, where movement of cations in the aqueous solution immediately adjacent to the negatively charged membrane surface may sweep fluid and certain membrane proteins along (McLaughlin & Poo, 1981). Proteins (Zagyansky & Jard, 1979; McLaughlin & Poo, 1981) and lipids, such as artificially incorporated fluorescent lipid 3,3'-dioctadecylindocarbocynine (Poo, 1981), may be moved in this way. Such movements occur over several minutes or tens of minutes when a steady lateral field of  $1 \text{ mV } \mu\text{m}^{-1}$  is applied.

A 'loose patch' voltage-clamp method, previously described (Stühmer & Almers, 1982; Almers, Stanfield & Stühmer, 1983), appears suitable for testing whether electrophoretic effects are possible in adult frog muscle. Lateral fields of the order of  $10 \text{ mV } \mu\text{m}^{-1}$  may be applied across the wall of the pipette. Since  $\text{Na}^+$  channels bear a large negative charge (Agnew, Levinson, Brabson & Raftery, 1978), lateral electric fields might be expected to move them into or out of the patch from which currents are recorded. This in turn would result in an increase or decrease in the amplitude of Na current. Thus changes in channel number would be recorded as changes in current amplitude.

We report here that changes in Na current of the expected time course and direction do take place when a steady potential is applied to the sarcolemma by means of a patch pipette. However, closer investigation reveals that these effects occur as a result of local membrane potential changes, and not because of lateral fields. It is concluded that the observed slow changes in Na current represent a slow inactivation process, with properties similar to one described for the node of Ranvier ('ultra-slow inactivation', Fox, 1976). Evidently  $\text{Na}^+$  channels cannot be moved even by substantial lateral fields. This finding is consistent with recent evidence that lateral mobility of  $\text{Na}^+$  channels is restricted (Stühmer & Almers, 1982; Almers, Stanfield & Stühmer, 1983). A preliminary account of this work has already appeared (Almers, Stanfield & Stühmer, 1981).

#### METHODS

*Patch voltage clamp.* The method used here is similar to that described previously (Almers *et al.* 1983). Na currents were recorded with a lightly fire-polished micropipette, filled with Ringer solution and having an internal tip diameter of 10–15  $\mu\text{m}$ , pressed against the sarcolemma (Fig. 1A). In most experiments, we used the sartorius muscle of the frog, *Rana temporaria*, but we also made a few measurements using the omohyoid muscle from rats freshly killed by exposure to an atmosphere of pure  $\text{CO}_2$ . In neither case was the muscle subjected to enzyme treatment, but surface connective tissue was removed as completely as possible by dissection.

The resistance of the pipettes used ( $R_p$ ) was generally between 0.5 and 0.8  $\text{M}\Omega$  and the resistance of the seal ( $R_s$ ) was of the order of 1  $\text{M}\Omega$ , giving a seal factor ( $A = R_s/[R_s + R_p]$ ) of 0.6–0.7.

As indicated in Fig. 1A, in most cases an arrangement of two Ag/AgCl electrodes was used to make contact with the Ringer solution in the pipette. One of these electrodes sensed the voltage while the other passed current, thus preventing the electrode polarization which might otherwise have resulted from steady currents over long periods. For the same reason, one Ag/AgCl bath electrode was used to sense the bath reference potential while a second such electrode connected the bath to ground.

*Mechanical stability.* We were able to record from patches of membrane over several hours. In order to do so, suction was applied continually to the inside of the pipette (50–100 cm H<sub>2</sub>O). As well as making the contact between pipette and membrane more stable, this procedure perhaps also facilitated consistent recordings by producing a steady flow of fresh Ringer solution over the patch. Additional mechanical stability was produced by coupling the electrode holder and amplifier head stage, itself held in a Huxley-designed manipulator, rigidly to the experimental chamber by allowing a heated liquid wax linkage to cool and solidify once the pipette had made contact with the muscle fibre. Lastly, experiments were carried out on a vibration isolation table.

*Recording of Na current.* As described before (Almers *et al.* 1983), once the bulk of leakage and capacitative current had been subtracted by analogue means, patch currents were passed through a 4-pole Bessel filter with a corner frequency of 5 kHz, and then sampled at 50 kHz using 12 bit A/D conversion. After digital subtraction of remaining leakage and capacitative currents (see Fig. 1B and below), Na currents were stored as groups of 244 samples in a NOVA 3 computer and written to disk. Peak values of Na currents were later measured by fitting a fourth order polynomial function to segments of the current records that were 0.5 to 1 msec long and included the peak. Currents are referred to the area of the circular patch covering the pipette orifice, whose inner diameter was measured with a 100× salt-water immersion objective (n.a. 1.2, Leitz).

*Pulse protocol and voltage convention.* Fig. 1B illustrates the pulse protocol used, actually giving the protocol for part of the experiment of Fig. 3. We used *pulse sequences* to measure the maximum Na current and separated these, each from the next, by a 10 sec long *pulse interval*. The pulse interval was itself used to apply steady potentials across the wall of the pipette, in an attempt to change the availability of Na current.

The pulse sequence contained a 4 msec depolarizing pulse, normally 80 mV in amplitude, which was used to measure the Na current. This depolarization followed a prepulse, 100 msec long, which hyperpolarized by 30 mV and whose function was to remove fast inactivation of Na channels. To complete subtraction of leakage and capacity currents, these pulses were themselves applied after four pulses and prepulses of the same duration but one quarter the amplitude. In Fig. 1B, these leakage- and capacity-current measuring pulses are shown superimposed on a 15 mV hyperpolarization to prevent their activating Na current. The currents during the four smaller pulses were added together and then subtracted from the currents during the final, larger pulse.

This pulse protocol was applied to the tip of the patch pipette (Fig. 1A, left). The potential at this point will be called  $V_t$  and expressed as the potential at the inside of the pipette relative to that of the bath. Thus negative values of  $V_t$  will depolarize the membrane of the patch (Fig. 1B, top trace). The amplitudes of pulses applied to the pipette were larger than the desired amplitude of  $V_t$  by a factor  $1/A$ . The value of  $A$  was determined by the computer (see Almers *et al.* 1983) just before the pulse interval began.

Fig. 1B (top trace) shows a potential change of  $-30$  mV applied across the rim of the pipette during the pulse interval. Such a change in  $V_t$  will, of course, also change the membrane potential of the patch. Therefore, in some experiments, a conventional two electrode voltage clamp was used to control independently the intracellular potential,  $V_i$  (Fig. 1). The micro-electrodes impaled the muscle fibre as close to the patch pipette as possible, and not more than three fibre diameters away. The voltage electrode was the closer to the pipette. The intracellular voltage clamp was used to cancel out the effect on the membrane potential of changes in  $V_t$  during the pulse interval. The appropriate command potential was supplied to the intracellular voltage clamp by a conventional square-wave generator, which was gated by digital output from our programmable wave form generator in order to insure that the change in  $V_i$  and the interpulse potential change were synchronized.  $V_i$  was returned to the holding potential while patch-current records were being made (Fig. 1B, middle trace). Using our convention, the membrane potential of the patch (Fig. 1B, bottom trace) is given by  $V_m = (V_i - V_t)$ .

In a number of experiments, however, we did not measure the resting potential of fibres from which we recorded. In such cases, the resting potential was inferred from the position of the  $h_\infty$  curve for conventional, fast Na inactivation (Hodgkin & Huxley, 1952) produced by 100 msec conditioning prepulses,

$$h_\infty = \{1 + \exp[(\bar{V} - V_P)/a]\}^{-1}, \quad (1)$$

where  $V_P$  is the value of  $V_t$  during the prepulse,  $\bar{V}$  the value of  $V_P$  at which  $h_\infty = 0.5$ , and  $a$  is determined by how steeply  $h_\infty$  varies with potential. (Note that depolarizing values of  $V_t$ ,  $V_P$  are

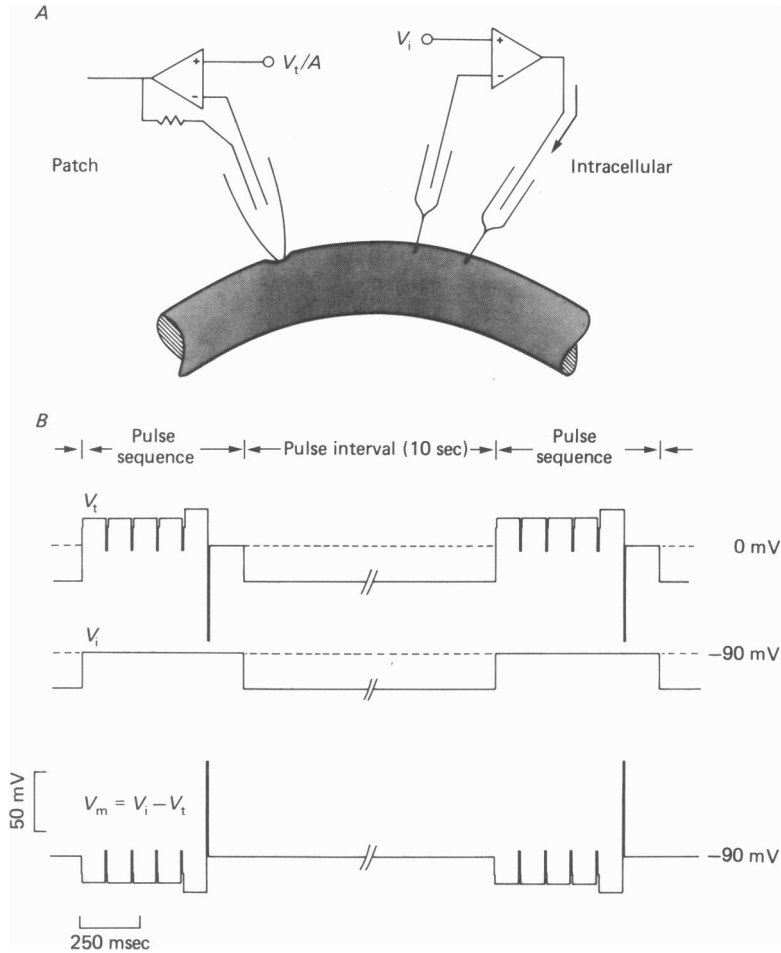


Fig. 1. *A*, schematic drawing of a muscle fibre and of the patch electrode (at left) and micro-electrodes used for the intracellular voltage clamp (at right). In the pipette, two Ag/AgCl electrodes were used, one to pass current and the other to sense voltage. The command pulse to the patch clamping amplifier was scaled by  $1/A$ , where  $A$  is the seal factor as defined in the text. Currents recorded by the patch amplifier were also scaled by multiplying by  $1/A$  to correct for loss of current to ground through the low resistance of the seal (see Almers *et al.* 1983). The intracellular clamp used 3 M-KCl and 2 M-K citrate filled micro-electrodes for recording internal potential and for passing current respectively. The intracellular clamp was used as indicated in the text. *B*, drawing of pulse sequence for measuring Na current, showing also the pulse interval during which steady potentials were applied to change the availability of Na channels. Each of four small pulses had exactly one quarter the amplitude of the fifth and larger pulse. The summed current during the four control pulses was subtracted from current during the fifth pulse in order to cancel out leakage and capacitive currents that had survived passage through an analogue leak and capacity subtractor. Sometimes the four small pulses were superimposed on a hyperpolarizing bias potential, as illustrated. A sixth and smaller pulse (not shown) was used to monitor ( $R_p + R_s$ ) and was applied just before the pulse interval. Voltages applied to the patch pipette are called  $V_t$  and given as the potential inside the pipette tip relative to the potential of the bath.  $V_i$  gives the potential of the inside of the fibre. The Figure illustrates a situation where the intracellular voltage clamp was used to compensate the potential applied with the patch pipette during the pulse interval. Such an arrangement avoids changes in membrane potential ( $V_m$ ) across the patch, except when leakage and Na currents were being measured.  $V_m$  (shown at the bottom of the Figure) is given by ( $V_i - V_t$ ). The pulse sequence shown was used as part of the experiment of Fig. 3.

given a negative sign here.)  $\bar{V}$  and  $a$  were chosen to give the best least-squares fit of eqn. (1) to the data. In muscle fibres from three frogs, we measured both the  $h_\infty$  relation with the patch pipette and the fibre resting potential ( $-93.5 \pm 0.8$  mV,  $n = 14$ ) with an impaling micro-electrode.  $\bar{V}$  was found to correspond to a membrane potential of  $-64.1 \pm 1.1$  mV, while  $a = 6.9 \pm 0.3$  mV ( $n = 14$ ). Where necessary, the membrane potential of the patch will be inferred from the potential at which  $h_\infty = 0.5$ . During long experiments,  $h_\infty$  relations were recorded at 1–2 hr intervals, and their position and steepness served to monitor constancy of the resting potential and stability of the fibre.

Except when measuring  $h_\infty$  relations, fast inactivation was completely removed by a 30 mV hyperpolarizing prepulse which was 100 msec long. A slower inactivation, recently described by Collins, Rojas & Suarez-Isla (1982), was also largely removed by the leakage- and capacity-current subtracting pulse sequence, which held the membrane at or negative to the resting potential for 525 msec before Na current was measured. This corresponds to about one time constant for recovery from slow inactivation.

*Solutions.* The frog Ringer solution contained (mM): NaCl, 115; KCl, 2.5; CaCl<sub>2</sub>, 1.8; and Na phosphate buffer (pH 7), 3. Rat Tyrode solution contained (mM): NaCl, 150; KCl, 3.5; MgCl<sub>2</sub>, 1; CaCl<sub>2</sub>, 2.5; glucose, 11; and HEPES (pH 7.5), 1 (Dulhunty, 1979). Experiments were carried out at temperatures between 10 and 18 °C.

## RESULTS

Fig. 2*A* shows records of Na and K current, measured with a pipette pressed against a muscle fibre, electrically isolating a patch of sarcolemma. The currents were elicited by depolarizing the patch in 10 mV steps by between 40 and 130 mV for periods of 4 msec. The largest Na current was recorded in response to an 80 mV depolarization and we shall use the current measured in response to such a step in potential as an assay for the number of functional Na channels present in the patch. Use of a depolarization of 80 mV also has the advantage that K channels are insufficiently rapidly activated to contribute substantially to the current measured within 4 msec (Fig. 2*B*), though larger depolarizations do activate significant K current.

*The effect of steady potentials applied to the patch pipette.* Fig. 2*B–D* shows the effect of a steady potential on this number of channels. The record shown in Fig. 2*B* was taken before and that in Fig. 2*C* approximately 17 min after the potential in the patch pipette was made 30 mV negative to that of the bath, during the intervals between pulses. The Na current declines to a low value and the time course of this decline is plotted as Fig. 2*D*. The effect was reversible (see later). As described in Methods the pulse protocol was designed to exclude both conventional, rapid inactivation and most of the slow inactivation recently described by Collins *et al.* (1982) as the cause of the decline.

The decline was not due to a change in the potential dependence of Na conductance, resulting in fewer of the available Na channels being opened by the test pulse. We tested for this possibility in one fibre where we measured current–voltage relations before and after Na current had been reduced by approximately one third by applying  $V_t = -20$  mV during the pulse interval. An 80 mV depolarization still produced the largest Na current, and no shift in potential dependence of Na conductance was recorded. Neither was the decline due to a shift of the voltage dependence of the inactivation parameter  $h_\infty$  (Hodgkin & Huxley, 1952) to more negative potentials. In one experiment, Na current had declined to one half under depolarization during the pulse interval. The  $h_\infty$  curve had shifted by less than 3 mV (see also Fig. 9) so

that the  $-30$  mV prepulse given before each Na current measurement is still expected to abolish conventional inactivation.

The change in the number of Na channels carrying current, which Fig. 2 indicates, could be due to the change in membrane potential during the pulse interval. But an alternative interpretation is that the reduction in Na current is brought about by

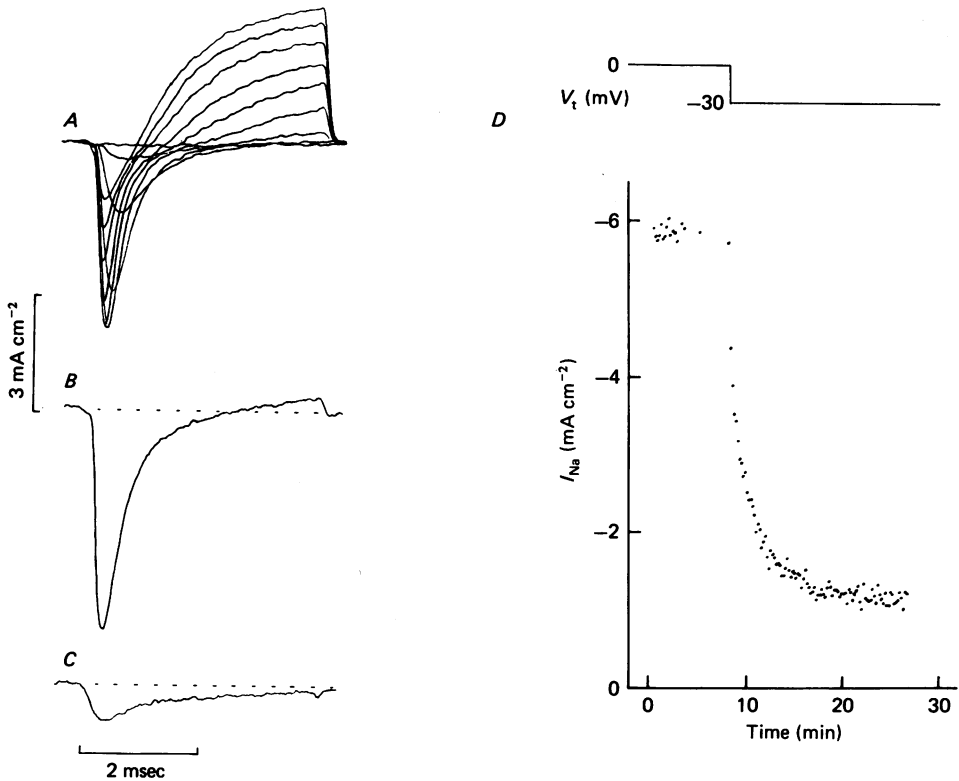


Fig. 2. *A*, records of Na and K currents obtained by depolarizing a membrane patch in 10 mV steps by from 40 to 130 mV. The currents are referred to the area of the orifice of the pipette. Depolarizing by 80 mV elicits the largest Na current, but is too brief to activate significant K current. *B* and *C*, records of Na current, recorded in response to an 80 mV depolarization, before (*B*) and 17 min after (*C*) the potential during the pulse interval was set to  $V_t = -30$  mV. No control of intracellular potential was used in this experiment, so the steady potential both depolarized the patch and applied a potential difference laterally across the rim of the pipette. *D*, time dependence of Na current in response to a potential applied during the pulse interval. Ordinate, peak  $I_{Na}$  during an 80 mV depolarization; abscissa, time (min). Temperature, 17 °C; internal diameter of patch electrode, 14  $\mu$ m; electrode resistance, 541 k $\Omega$ ; fibre no. 3010.

the lateral field present across the rim of the pipette. The width of the annular zone of sarcolemma in contact with the pipette is not known with certainty, but we believe that it is less than 10  $\mu$ m across. Thus for a steady potential of  $-30$  mV in the pipette, the zone will experience a lateral field  $> 3$  mV  $\mu$ m<sup>-1</sup>. Since the Na-channel protein is known to bear a large negative charge, the field may sweep channels away from the patch, depleting the contact zone. Channels may then move from the patch into

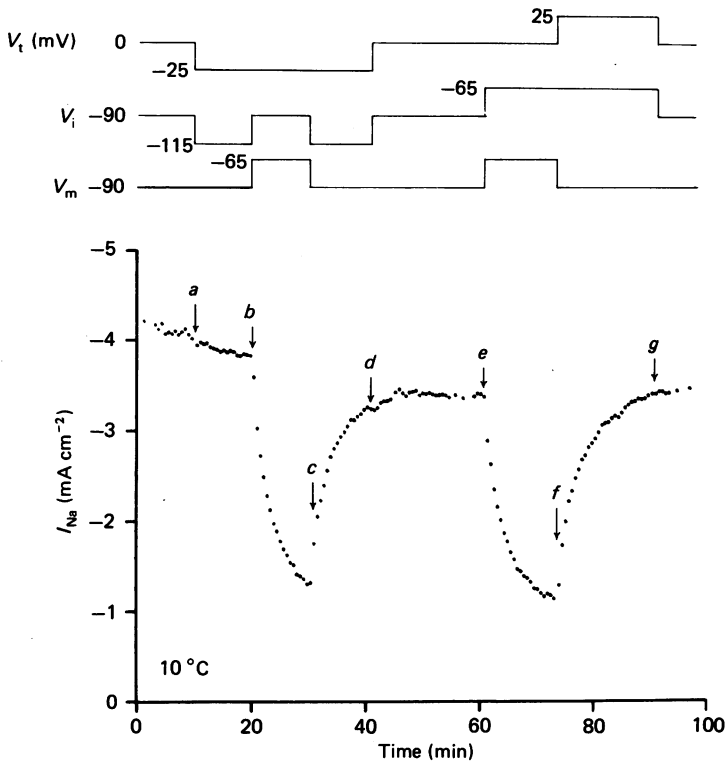


Fig. 3. Changes in Na current density depend on changes in membrane potential, not on lateral fields. Patch recording was coupled with an intracellular voltage clamp as illustrated in Fig. 1. At the top are shown the potentials applied during the pulse interval to the patch pipette ( $V_t$ ), at the intracellular recording electrode ( $V_i$ ) and consequently across the membrane ( $V_m$ ). Below, peak  $I_{Na}$  ( $\text{mA cm}^{-2}$ , ordinate), in response to a depolarization to  $-10$  mV, is plotted against time (min, abscissa), showing that changes in Na current follow changes in  $V_m$ , not  $V_t$  alone. The markers *a-g* indicate the times of change of the potentials illustrated above. At *a*, *d* and *g*, changes in  $V_t$  were compensated by changes in  $V_i$  so that only lateral fields were applied (*a*) or removed (*d*, *g*). Depolarization of the patch membrane (*b*, *e*) resulted in the decline in current density whether a lateral field was present (*b*) or not (*e*). Recovery occurred under repolarization (*c*, *f*) whether the potential inside the pipette was negative (*c*) or positive (*f*) with respect to the potential of the bath.

Temperature,  $10^\circ\text{C}$ ; internal diameter of patch electrode,  $22\ \mu\text{m}$ ; pipette resistance,  $670\ \text{k}\Omega$ ; fibre no. 4021.

the contact zone by lateral diffusion and be pulled out of the zone by the electric field. This process could continue until only few channels are left in the patch. Loss of Na current, as shown in Fig. 2*D*, might, then, result from a combination of 'lateral electrophoresis' and lateral diffusion of channels.

*Changes in the number of functional Na channels depends on changes in membrane potential.* The second possibility may be removed by an experiment of the kind illustrated in Fig. 3. Here both patch and intracellular voltage clamps are used to apply lateral fields in the absence of changes in membrane potential or changes in membrane potential in the absence of a lateral field. The potentials applied during

the pulse interval to the patch electrode ( $V_t$ ) and with the intracellular voltage clamp ( $V_i$ ) are illustrated at the top of Fig. 3 as are the resulting values of  $V_m$ . The markers  $a-g$  on the plot of Na current against time indicate when changes are made in  $V_t$ ,  $V_i$ , or both.

Substantial reductions in Na current occur only when membrane potential is changed, and these reductions are similar both as regards size and rate whether a lateral field is present across the pipette rim (Fig. 3*b*) or not (Fig. 3*e*). The loss of Na current appears to follow an exponential time course with rate constants ( $1/\tau$ ), computed from least-squares fits of the transients to the function

$$I_{\text{Na}}(t) = I_{\text{Na}}(\infty) - \{I_{\text{Na}}(\infty) - I_{\text{Na}}(0)\} \exp(-t/\tau), \quad (2)$$

of 0.278 and 0.283  $\text{min}^{-1}$ , respectively. In eqn. (2),  $I_{\text{Na}}(0)$  and  $I_{\text{Na}}(\infty)$  are the initial and steady-state values of  $I_{\text{Na}}(t)$  and  $t$  is the time since the last change in potential during the pulse interval.

Recovery of Na conductance occurs (Fig. 3*c, f*) when the membrane is repolarized, and does so at a very similar rate whether  $V_t$  is negative (Fig. 3*c*; rate constant for recovery 0.290  $\text{min}^{-1}$ ) or whether  $V_t$  is positive (Fig. 3*f*; rate constant 0.231  $\text{min}^{-1}$ ) indicating that lateral fields do not alter the process.

Lateral fields by themselves (Fig. 3*a, d, g*) have little or no effect although a small reduction in current amplitude appears to follow the change in  $V_t$  from 0 to  $-25$  mV shown at  $a$  in Fig. 3. This reduction could, however, be explained by failure to compensate perfectly with the intracellular clamp for changes in membrane potential produced by applying a potential to the patch electrode.

The completeness of the compensation was assessed by using the patch electrode to measure  $h_\infty$  relations under conditions where the holding potential was changed with the intracellular clamp. With the intracellular holding potential at  $-90$  mV, the half point of the  $h_\infty$  curve was at  $-65$  mV. When the intracellular holding potential was changed to  $-110$  and to  $-130$  mV, the half point of the  $h_\infty$  curve appeared to change to  $-68$  and  $-71$  mV, respectively. This observation suggests that the membrane of the patch experienced approximately only 17 mV out of a 20 mV change at the intracellular voltage electrodes so that a 3–4 mV depolarization actually occurred at  $a$  in Fig. 3. The steepness factor,  $a$  of eqn. (1), remained unchanged at 6.7 mV.

In summary, the result of Fig. 3 shows that slow changes in Na current result from changes in membrane potential. Apparently, Na channels of sarcolemma are able to undergo a very slow inactivation process. The result further suggests that if electrical fields applied across the rim of the pipette are able to move Na channels laterally in the membrane, any resulting change in their density is too small to be easily measurable, at least within the time scale of our experiments (see also Fig. 9).

Similar very slow changes in Na conductance were elicited by the same pulse regime applied to a single muscle fibre dissected from the semitendinosus of the frog and voltage clamped using the vaseline-gap method (Hille & Campbell, 1976; Almers & Palade, 1981). The ends of this fibre were cut in a phosphate-buffered CsF (120 mM) solution.

*Potential and time dependence of slow changes in the size of Na currents.* Since the patch method allows recording over long periods, we investigated the potential and time dependence of changes in the amplitude of Na current in three fibres in a reasonably complete way. The result of one such experiment is shown in Fig. 4, which



illustrates the values of  $V_m$  applied during the pulse interval and the resulting changes in Na-current density. The fibre resting potential was taken to be  $-89$  mV from the half point of  $h_\infty$  relations measured at times marked by arrows in Fig. 4.

The size of the Na currents measured falls under depolarization and recovers during repolarization. Hyperpolarization during the pulse interval sometimes produces a small increase in current amplitude. These changes in current density follow a very slow time-scale, taking many minutes to come to completion at a given potential.

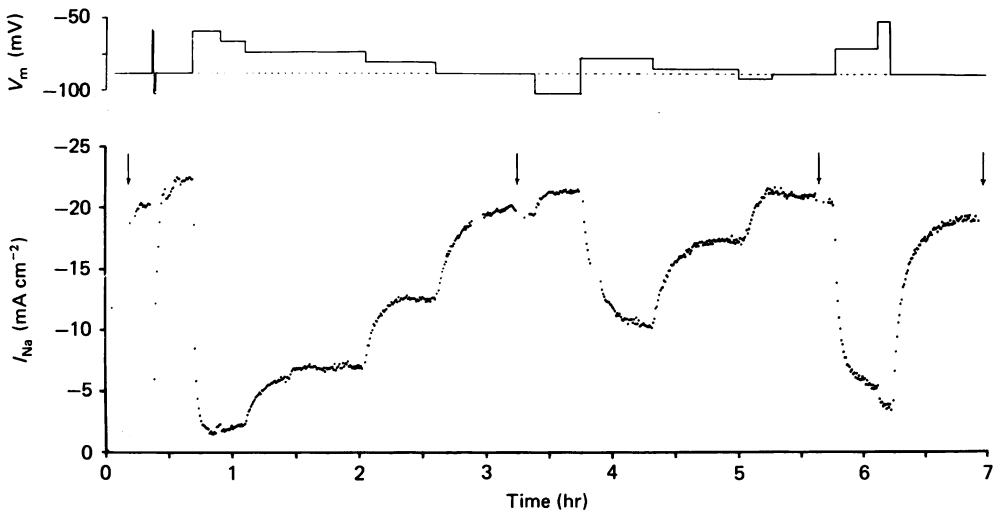


Fig. 4. Effect on Na current amplitude of steady potentials applied between pulses. The potentials applied during the pulse interval to the membrane of the patch ( $V_m$ ) are shown at the top of the Figure. Below, the amplitude of the Na current, measured in response to an 80 mV depolarization (mA cm<sup>-2</sup>; ordinate), is plotted against the time elapsed since the first record was taken (hr; abscissa). Vertical arrows in the lower part of the Figure indicate when the condition of the fibre was checked by measuring  $h_\infty$  relations. From left to right the depolarizations necessary to give  $h_\infty = 0.5$  were by 24.4, 25.3, 26.6, and 23.4 mV. The mean value was 24.9 mV, so resting potential was taken to be  $-89$  mV (see Methods). Temperature, 17 °C; internal diameter of patch electrode, 10  $\mu$ m; electrode resistance, 535 k $\Omega$ ; fibre no. 3003.

*Long-term dependence of Na conductance on membrane potential.* Fig. 5 illustrates the dependence in the steady state of the amplitude of Na currents on the membrane potential during the pulse interval, giving the results for three fibres. In constructing this relation, we have expressed the currents measured in the steady state as a fraction of those obtained in the steady state when a 20 mV hyperpolarization was applied between pulses. The results indicate that although nearly all the Na conductance is available at the resting potential, Na conductance begins to fall with even quite small depolarizations. Only about one half is available at a membrane potential of  $-76$  mV, as judged by fitting the experimental points to the function given in the legend to Fig. 5.

*Time course of slow changes in Na-current amplitude.* The steady-state values of the density of Na current plotted in Fig. 5 were obtained by fitting segments of our experimental results to the exponential function given above (eqn. 2).

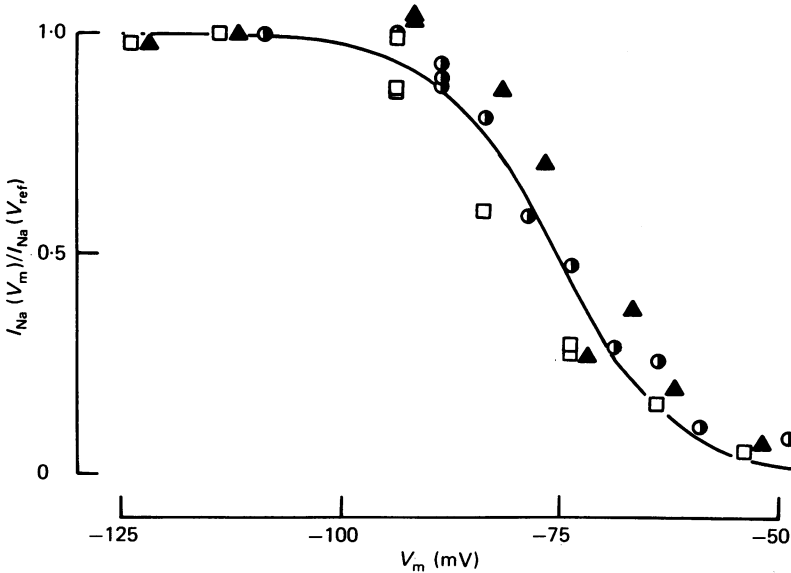


Fig. 5. Equilibrium availability of Na current as a function of membrane potential. The ordinate gives the peak Na current as a fraction of that obtained when the membrane of the patch was hyperpolarized by 20 mV ( $V_{ref}$ ); abscissa, membrane potential (mV).  $\square$ , fibre no. 1140; resting potential (r.p.),  $-94$  mV;  $T$ ,  $14$  °C; internal diameter of patch electrode,  $18$   $\mu$ m; resistance of patch electrode,  $618$  k $\Omega$ .  $\bullet$ , fibre no. 3003; for details of the fibre, see legend to Fig. 4.  $\blacktriangle$ , fibre no. 3010; for details of the fibre see legend to Fig. 3; r.p.,  $-92$  mV. The antipolarization arrangement (Fig. 1A) was used in both fibres no. 3003 and no. 3010 but not in fibre no. 1140. The continuous line gives a least-squares fit to the function  $I_{Na}(V_m)/I_{Na}(V_{ref}) = \{1 + \exp [(V_m - V_b)/b]\}^{-1}$  where  $V_b = -76$  mV and  $b = 6.7$  mV.

Examples of the results of fitting segments of the experiment of Fig. 4 are shown in Fig. 6. Fig. 6A, B shows that when the potential during the pulse interval is sufficiently negative ( $V_m = -69$  and  $-79$  mV, respectively) the time course of the change in the size of Na currents fits the exponential function closely. However, when the membrane potential between pulses is made more positive (Fig. 6C, D), a more rapid change in Na current occurs and is seen as a step in the size of the Na current when the potential changes at  $t = 0$ . The simplest explanation of the initial step in current amplitude is that it is due to the presence of an inactivation process (Collins *et al.* 1982), intermediate between conventional, fast inactivation and the very slow process described here, and that this process is not completely removed before the Na current is measured.

The relation between the rate constants for loss or recovery of Na currents and membrane potential is shown in Fig. 7A. Rate constants are smallest at potentials close or slightly positive to resting potential where they are of the order of  $0.1$   $\text{min}^{-1}$ . They are higher at both hyperpolarized and more depolarized levels. Further, they do not appear to be strongly dependent on whether Na current is decreasing or increasing with time (Fig. 7A).

These rates for the loss and recovery of Na conductance are likely to be slight underestimates since the membrane spends only about 94% of the time at the inactivating potential, which is applied during the pulse interval. Little error will

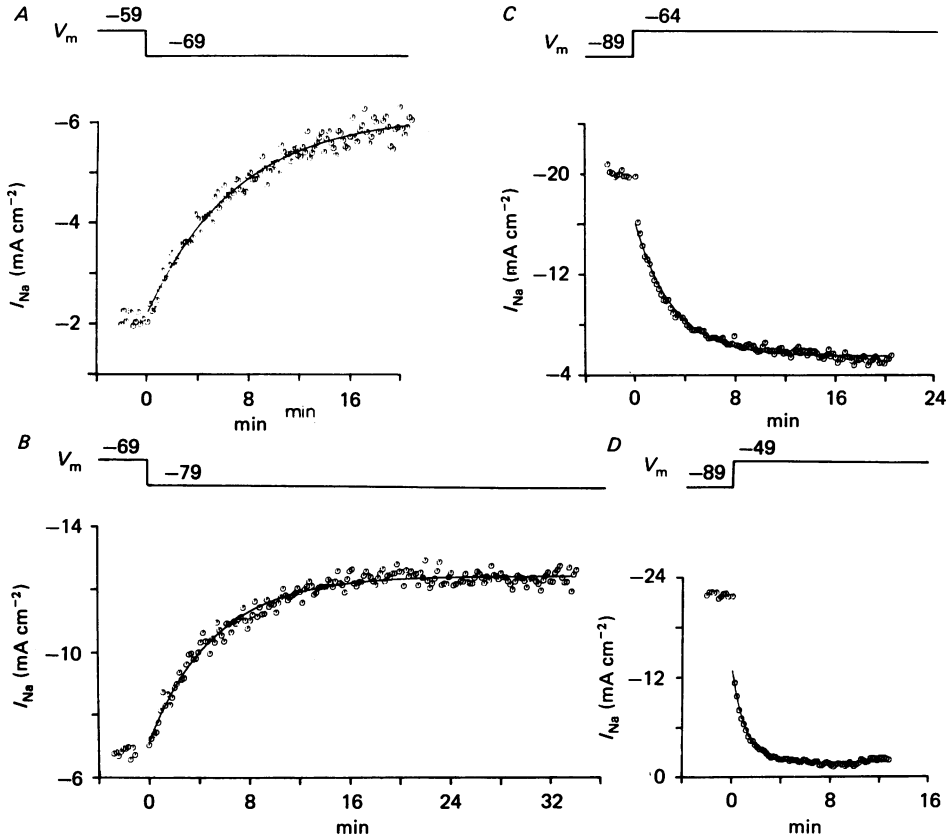


Fig. 6. Changes in Na current as a consequence of changes in membrane potential applied during the pulse interval. In each case Na current (ordinate) is plotted against time (abscissa). *A*, repolarizing from  $-59$  to  $-69$  mV; *B*, from  $-69$  to  $-79$  mV. *C*, depolarizing from  $-89$  to  $-64$  mV; and *D*, from  $-89$  to  $-49$  mV. The ten left-hand points in each graph give Na currents measured during the pulse interval before the membrane potential was changed. The lines were drawn to the points to give the best fit to  $I_{\text{Na}}(t) = I_{\text{Na}}(\infty) - \{I_{\text{Na}}(\infty) - I_{\text{Na}}(0)\} \exp(-t/\tau)$  with  $1/\tau = 0.141$  (*A*);  $0.191$  (*B*);  $0.330$  (*C*); and  $0.887 \text{ min}^{-1}$  (*D*). Records from fibre no. 3003 (see Fig. 4).

result from recovery occurring during the pulse sequence used to measure Na current, however, since the rate constant for recovery at the resting potential is of the order of  $0.1 \text{ min}^{-1}$  and the pulse sequence for measuring Na current takes only 600 msec (Fig. 1*B*).

*Steady-state potential dependence of the inactivation process.* Fig. 7*B* illustrates the membrane potential dependence of the very slow inactivation process described here. We have taken  $(1-u)$  to represent the fraction of Na channels in this inactivated state at a given potential and time, so that the points ( $\blacktriangle$ ) have been plotted as  $u_{\infty}$ . They have also been corrected for the presence of an intermediate inactivation process (Collins *et al.* 1982), the inset showing the method we used to make the correction.

In order to obtain the value of  $u_{\infty}$  at a given potential, we assumed that the intermediate inactivation process had reached its steady state within one pulse interval (10 sec) after changing  $V_m$ . We could therefore use eqn. (2) to fit subsequent points by a least-squares method, so predicting

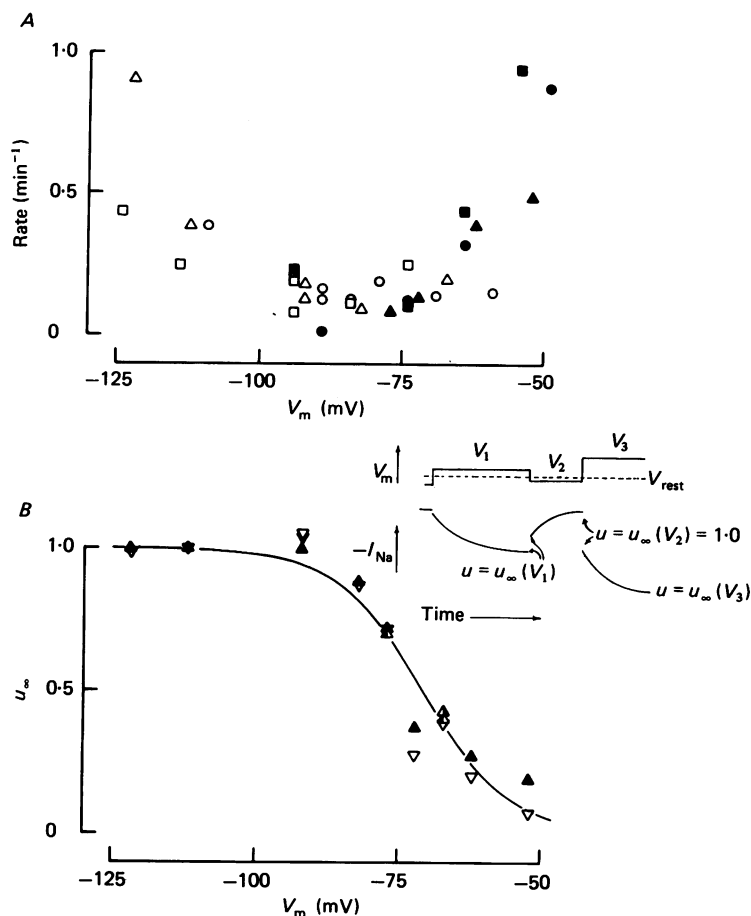


Fig. 7. *A*, rate constants for development (open symbols) and recovery (filled symbols) from slow inactivation, plotted against membrane potential. Rate constants were obtained by fitting eqn. (2) to data.  $\square$ ,  $\blacksquare$  fibre no. 1140;  $\circ$ ,  $\bullet$  fibre no. 3003;  $\triangle$ ,  $\blacktriangle$  fibre no. 3010. *B*, steady-state relationship between slow inactivation and membrane potential. The variable  $u(\infty)$  is unity when all Na channels are active, and zero when all channels have succumbed to slow inactivation.  $\nabla$ , values from Fig. 5;  $\blacktriangle$ , values corrected for an inactivation process of intermediate time course (the 'step' in Fig. 6*C, D*).  $\blacktriangle$ ,  $\blacktriangle$  were obtained from the same transient using two different reference measurements for normalization. The line is drawn according to  $u_\infty = \{1 + \exp [(V_m - \bar{V}_u)\nu]\}^{-1}$  as described in the text.  $\bar{V}_u = -71$  mV,  $\nu = 7.7$  mV. Fibre no. 3010. *Inset* illustrates the method of correcting for an intermediate inactivation process, which is assumed to equilibrate within a single pulse interval. Exponentials are fitted to all data points except the one at  $t = 0$ , i.e. the one immediately preceding a change in interpulse potential. The value of  $u(t = 0)$  is defined by the value of the fitted curve at the moment of potential change. For normalization, steady values of current at a given potential were divided by the most closely preceding or following measurement of steady current at a potential equal or negative to the resting potential (such as  $V_2$ ), where  $u_\infty = 1.0$  was assumed.

an initial value of  $I_{\text{Na}}$  corresponding to the initial value of  $u$ . This initial value of  $u$  will itself be equal to the old steady-state value, reached at the membrane potential previously applied during the pulse interval.

In the fibre in which we corrected for the intermediate inactivation process, the Na current reached saturating amplitudes at potentials equal or negative to the resting potential. We were thus able to regard such potentials as reference potentials at which  $u_{\infty} = 1.0$ . In this fibre, the experiment was designed so that measurements of  $u_{\infty}$  were made at not more than two consecutive depolarizing levels before  $V_m$  was returned to such a reference level. In the inset of Fig. 7, as an example,  $V_2$  gives a reference potential, so that for  $V_3$ ,  $u_{\infty}(V_3) = I_{\text{Na}}(0)/I_{\text{Na}}(\infty)$ , where  $I_{\text{Na}}(0)$  and  $I_{\text{Na}}(\infty)$  are the initial and steady-state amplitudes of Na current *calculated* by fitting eqn. (2) to experimental points obtained for  $V_3$  at  $t > 0$ .

In fact the correction makes relatively little difference to the final result as Fig. 7B shows. The corrected points in Fig. 7B ( $\blacktriangle$ ) are fitted by a least-squares method to the function:

$$u_{\infty} = \{1 + \exp [(V_m - \bar{V}_u)/\nu]\}^{-1}, \quad (3)$$

where  $u_{\infty}$  is 0.5 at membrane potential ( $V_m$ ) of  $\bar{V}_u = -71$  mV, while  $\nu = 7.7$  mV. The corrected relation has a half point at a potential 2 mV less negative than does the best fit of eqn. (3) to the uncorrected values ( $\nabla$ ) for this fibre, and it is slightly less steep in its dependence on membrane potential.

*Slow inactivation processes in rat muscle.* We carried out a few experiments on the omohyoid muscle of the rat to see whether a similar inactivation process was present in mammalian muscle fibres. On first making a seal onto rat muscle fibres, Na currents were small, probably because the resting potential of the fibre, measured with an intracellular micro-electrode, was between  $-70$  and  $-80$  mV. However, we were able to recover a substantial amount of Na current by applying a hyperpolarizing holding potential to the pipette. Our results show that slow inactivation is present and that it occurs at much the same rate as, or a little faster than, in the frog at the same temperature. While these results are less complete than those for frog muscle, they show that the range of membrane potentials over which the very slow changes in Na conductance occurred was between about  $-60$  and  $-100$  mV.

Fig. 8 summarizes results from a fibre investigated with the patch clamp. The currents, shown in the inset to the Figure were obtained by depolarizing the patch in 10 mV steps to between  $-83$  mV and  $+37$  mV. The patch was otherwise held at  $-103$  mV. Also shown are the effects of applying steady potentials during the pulse interval, which resulted in loss and recovery of Na current, as in frog. When the patch was depolarized to  $-73$  mV there was a marked and rapid loss of Na current. This was followed by a very slow inactivation of Na current which occurred with a rate constant of  $0.478 \text{ min}^{-1}$ .

*The potential dependence of rapid inactivation in frog muscle and lateral electrophoresis.* Our results suggest that Na channels do not easily move laterally in the membrane of frog muscle fibres under the influence of an electrical field applied across the rim of a patch pipette, but that very slow changes in current amplitude occur which depend on membrane potential. However, even if movement of Na channels themselves cannot be detected, it is possible that movement of other constituents of the membrane, which might affect channel function, can be. For example, if charged phospholipids could be moved laterally this might result in changes in surface

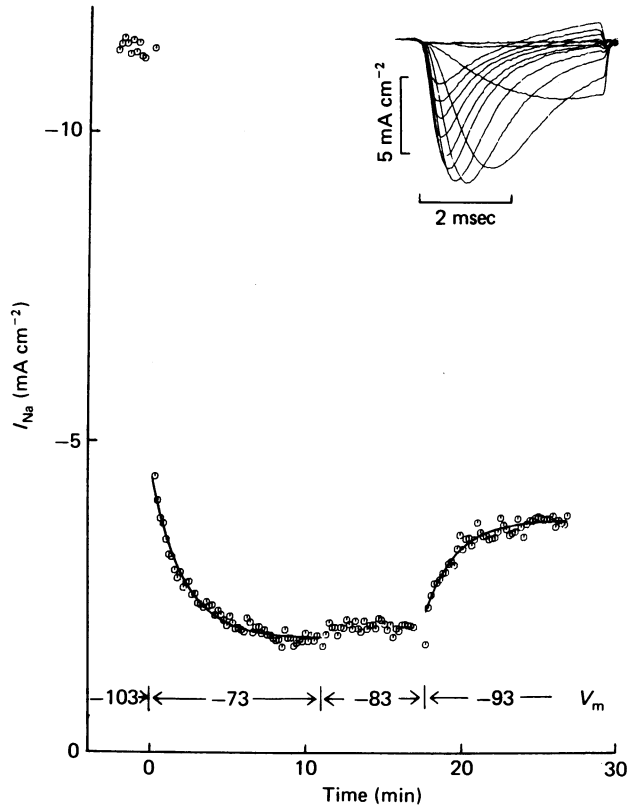


Fig. 8. Experiment using omohyoid muscle of rat. Inset gives records of currents obtained with depolarizations in 10 mV steps to from  $-83$  mV to  $+37$  mV. The plot shows the effect on amplitude of Na current (ordinate) of applying steady potentials during the pulse interval to the patch pipette, with the resulting membrane potentials shown below the plot. Abscissa gives time. The lines to the points were fitted to eqn. (2) of text, with  $1/\tau = 0.478 \text{ min}^{-1}$  at  $-73$  mV and  $0.496 \text{ min}^{-1}$  at  $-93$  mV. The resting potential of the fibre was measured as  $-73$  mV at the end of the experiment and, in this fibre, all pulses were superimposed on a 30 mV hyperpolarizing holding potential applied with the patch pipette. Fibre no. 1RSI; temperature,  $10^\circ\text{C}$ ; electrode internal diameter,  $11 \mu\text{m}$ ; electrode resistance,  $600 \text{ k}\Omega$ .

potential which in turn could shift the potential dependence of the rapid inactivation of Na current.

We examined this possibility in a fibre under patch and intracellular voltage clamps. During all pulse intervals the intracellular clamp held the potential across the membrane patch at  $-100$  mV in order to avoid complications due to slow inactivation processes. Shifts in the potential dependence of a rapid inactivation were monitored by varying the potential during a 100 msec prepulse which preceded the brief depolarization to  $-10$  mV used to elicit Na current. The prepulse potential alternated between  $-30$  mV and  $29$  mV, where the former ensured that  $h_\infty = 1$ , and the latter was chosen to set  $h_\infty$  to about 0.5. The ratio of Na currents recorded by this regime of pulse pairs (current with a  $29$  mV prepulse divided by current with a  $-30$  mV prepulse) gives the value of  $h_\infty$  at  $-71$  mV as a function of time.

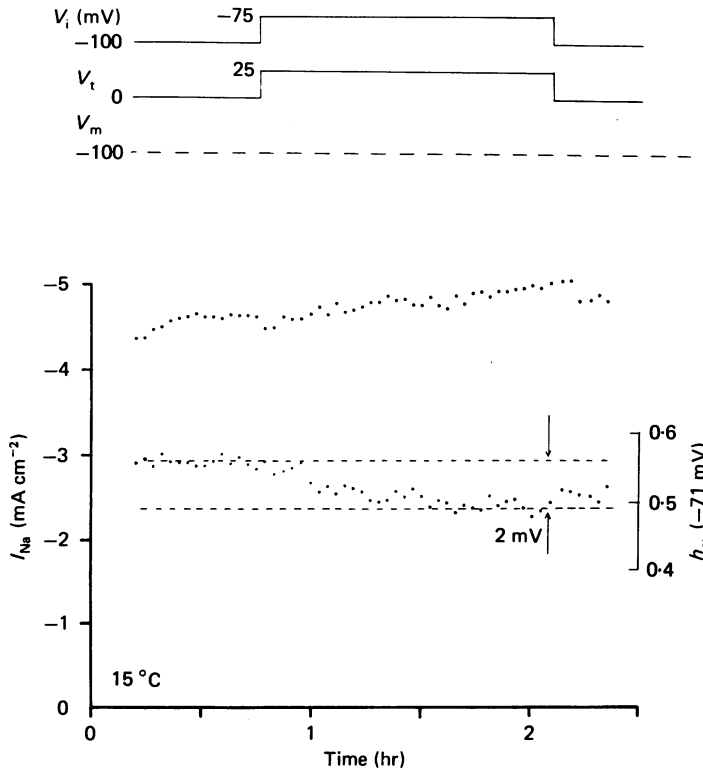


Fig. 9. Potential dependence of rapid inactivation is not altered by applying a lateral field. Both intracellular voltage clamp and patch recording are used. Steady potentials, applied during pulse intervals, are shown at the top for internal ( $V_i$ ), pipette ( $V_t$ ) and membrane potentials ( $V_m$ ). Below, the Na current (upper set of points, left-hand ordinate) and the value of  $h_\infty$  at  $V_m = -71$  mV (lower set of points, right-hand ordinate) are plotted against time (abscissa).  $h_\infty$  was measured by expressing the Na current obtained after application of a 100 msec prepulse to  $-71$  mV as a fraction of that obtained after a 100 msec prepulse to  $-130$  mV. The horizontal dashed lines in the lower part of the Figure indicate the change in the value of  $h_\infty$  if its potential dependence shifted by 2 mV. Fibre no 5003; temperature,  $15^\circ\text{C}$ ; internal diameter of electrode,  $12.5\ \mu\text{m}$ ; electrode resistance,  $630\ \text{k}\Omega$ .

The experiment is illustrated in Fig. 9 (lower trace). As in the preceding experiments, Na currents were elicited at 11 sec intervals (see Fig. 1*B*). Evidently  $h_\infty$  ( $-71$  mV) changed little during the 100 min that a potential difference was applied laterally across the rim of the patch pipette. From the shape of  $h_\infty$  relations measured in this fibre, the result corresponds to a shift in the potential dependence of  $h_\infty$  by no more than 2 mV. Similar results were observed in a further two fibres. Either the surface charge due to membrane lipids does not influence Na channel inactivation, or the lipids immediately surrounding the Na channel are restricted in their mobility. The upper trace in Fig. 9 shows current with  $-30$  mV prepulses only. It indicates that a lateral potential difference of  $V_t = 25$  mV applied for 100 min did not significantly change the number of functional Na channels in the patch, confirming that the lateral distribution of Na channels is not readily altered by an electric field.

## DISCUSSION

'Ultra-slow' inactivation in skeletal muscle. This paper shows that a steady depolarization applied to a patch of sarcolemma can reversibly diminish the Na current that can be recorded by applying a test depolarization of standard amplitude. The observed changes occur with time constants of 1–10 min, and are not due to changes in the inactivation and activation gating parameters  $m$  and  $h$  (Hodgkin & Huxley, 1952). Neither are they due to lateral redistribution of Na channels possibly caused by the lateral electric field (Poo, 1981) expected where the rim of the pipette contacts the sarcolemma. Instead, they probably reflect a 'slow inactivation' of Na channels, that is, a membrane potential-dependent change of state that renders Na channels temporarily non-conducting.

Slow inactivation processes have been described before. In lobster (Narahashi, 1964), squid (Adelman & Palti, 1969; Rudy, 1978), and *Myxicola* giant axons (Schauf, Pencek & Davis, 1976; Rudy, 1981), as well as in myelinated nerve (Peganov, Khodorov & Shishkova, 1973; Brismar, 1977), and in frog skeletal muscle (Collins *et al.* 1982), cell membrane depolarization maintained over hundreds of milliseconds results in the reversible decline of Na current. Though slower than the rapid inactivation occurring during a single action potential (Hodgkin & Huxley, 1952), these processes are still 2–3 orders of magnitude faster than the effects described here. Results similar to ours were obtained on myelinated nerve by Fox (1976) who introduced the term 'ultra-slow inactivation.'

As we demonstrate here, ultra-slow inactivation becomes prominent if the resting potential falls into the range  $-70$  to  $-80$  mV, and once it has occurred, recovery of electrical excitability may take many minutes. Prolonged depolarizations may be produced locally by depolarizing blockers of the neuromuscular junction, such as suxamethonium or decamethonium (see, for example, Taylor, 1980). Generalized long-lasting depolarizations are associated with hypokalaemic periodic paralysis of muscle (for example Gordon & Kao, 1978). The physiological role of ultra-slow inactivation is not clear at this point, though the possibility that some inactivation is present at the resting potential in mammalian muscle may deserve further attention. Slow inactivation processes will presumably alter the ability of muscle fibres to fire repetitive action potentials, as in certain nerve fibres (Rudy, 1981), and will, for example, almost certainly help terminate repetitive discharge occurring in myotonic states (Adrian & Bryant, 1974).

Onset of, and recovery from, ultra-slow inactivation follow exponential time courses. In this sense our result differs from that of Fox (1976) who, when he first demonstrated such inactivation in myelinated nerve, fitted its development with a double exponential. Neumcke, Fox, Drouin & Schwarz (1976) suggested that the process depended on electrodiffusion of a charged substance, supposed to control Na permeability, transversely across the membrane. They therefore fitted the onset of the inactivation to an error function. However, Brismar (1977) found evidence for a slow inactivation process whose time course was similar to the faster exponential described by Fox (1976). Our interpretation is similar to Brismar's (1977), namely that there exists in sarcolemma, as in nerve membranes, separable slow and very slow inactivation processes for Na channels. However, our results do not allow us to comment on the relation between fast, slow, and ultra-slow inactivation steps.



*Lateral movement by electrophoresis.* While our results rule out the possibility that ultra-slow inactivation depends on the lateral movement of Na channels, they also suggest that little such movement occurs. Indeed, while the decline in Fig. 3*a* and the small and very slow increase in Na current seen in Fig. 9 when  $V_t$  was made positive by 25 mV are in the direction expected for electrophoresis of a protein with a negative charge (Agnew *et al.* 1978), they are much smaller and slower than expected if Na channels redistributed as readily as concanavalin A or  $\alpha$ -bungarotoxin receptors in embryonic *Xenopus* muscle cells (Poo, Poo & Lam, 1978; Orida & Poo, 1978).

As discussed in a previous paper (Stühmer & Almers, 1982), failure to move cannot be due to the proximity of the pipette rim and the sarcolemma. With the relatively loose seal the probable distance between pipette and membrane is 100–200 nm, as computed from seal resistance, pipette diameter, and resistivity of frog Ringer solution. The possibility that we fail to see movement because electro-osmotic and electrophoretic effects just balance each other (see, for example, Poo, 1981; McLaughlin & Poo, 1981) is more difficult to remove, and we have not pursued this possibility, given the presence of a potential-dependent process for which it is difficult to correct with the required accuracy (as in the experiment of Fig. 3). However, recent evidence suggests that Na channels cannot readily move in the sarcolemma by diffusion, the diffusion coefficient being less than  $1$  to  $2 \times 10^{-12}$  cm<sup>2</sup> sec<sup>-1</sup>. This evidence is first that local destruction of channels by U.V. light is not followed by repopulation from adjacent areas of membrane (Stühmer & Almers, 1982) and secondly that channels can be shown to be less evenly distributed over the sarcolemma than might be expected from their molecular size and lifespan in the membrane (Almers *et al.* 1983). Immobility would explain the observed failure of Na channels to redistribute under an electric field.

Our experiments also showed that applying lateral fields did not strongly alter the potential dependence of fast inactivation of Na channels, as they might if charged phospholipids could be moved in the membrane by a lateral electric field. A 25–30 mV p.d. applied across the pipette rim for 30–100 min causes only a small (< 3 mV) shift of the  $h_\infty$  curve to more negative potentials. Although the shift is in the right direction, it is by much less than the potential applied. Perhaps the lipid molecules near the Na channel are rendered immobile by chemical interaction with hydrophobic regions of the channel protein. Alternatively, lipids may be freely mobile, but unable to influence channel gating. Since the probable radius of the Na channels (2 nm, Ellisman, Agnew, Miller & Levinson, 1982) is larger than the Debye length in frog Ringer (1 nm) it seems possible that surface charges carried by membrane phospholipids may not much affect the voltage dependence of Na conductance, which may be controlled by site(s) buried deep inside the Na channel protein (see, for example, Armstrong, 1981).

In summary, our experiments show that an ultra-slow inactivation of Na conductance is present in skeletal muscle fibres. There is little sign that lateral electric fields cause lateral motion of Na channels or of membrane components influencing Na channel gating.

We thank Lea Miller and Judy Lewis for their expert preparation of this manuscript. P.R.S. received a travel grant from the Wellcome Trust and W.S. held a post-doctoral fellowship from the Max Kade Foundation. Supported by USPHS grant no. AM-17803 and the Muscular Dystrophy Association of America Inc.

## REFERENCES

- ADELMAN, W. J. & PALTÍ, Y. (1969). The effects of external potassium and long duration voltage conditioning on the amplitude of sodium currents in the giant axon of the squid, *Loligo pealei*. *J. gen. Physiol.* **54**, 589–606.
- ADRIAN, R. H. & BRYANT, S. H. (1974). On the repetitive discharge in myotonic muscle fibres. *J. Physiol.* **240**, 505–515.
- AGNEW, W. S., LEVINSON, S. R., BRABSON, J. S. & RAFTERY, M. A. (1978). Purification of the tetrodotoxin-binding component associated with the voltage-sensitive sodium channel from *Electrophorus electricus* electroplax membranes. *Proc. natn. Acad. Sci. U.S.A.* **75**, 2606–2610.
- ALMERS, W. & PALADE, P. T. (1981). Slow calcium and potassium currents across frog muscle membrane: Measurements with a vaseline-gap technique. *J. Physiol.* **312**, 159–176.
- ALMERS, W., STANFIELD, P. R. & STÜHMER, W. (1981). Lateral mobility and distribution of sodium channels in frog muscle membrane. *Abstracts of the VII International Biophysics Congress and III Pan-American Biochemistry Congress, Mexico City*, p. 303.
- ALMERS, W., STANFIELD, P. R. & STÜHMER, W. (1983). Lateral distribution of sodium and potassium channels in frog skeletal muscle: Measurement with a patch clamp technique. *J. Physiol.* **336**, 261–284.
- ARMSTRONG, C. M. (1981). Sodium channels and gating currents. *Physiol. Rev.* **61**, 644–683.
- BRISMAR, T. (1977). Slow mechanism for sodium permeability inactivation in myelinated nerve fibre of *Xenopus laevis*. *J. Physiol.* **270**, 283–297.
- COLLINS, C. A., ROJAS, E. & SUAREZ-ISLA, B. A. (1982). Activation and inactivation characteristics of the sodium permeability in muscle fibres from *Rana temporaria*. *J. Physiol.* **324**, 297–318.
- DULHUNTY, A. F. (1979). Distribution of potassium and chloride permeability over the surface and T-tubule membranes of mammalian skeletal muscle. *J. Membrane Biol.* **45**, 293–310.
- ELLISMAN, M. H., AGNEW, W. S., MILLER, J. A. & LEVINSON, S. R. (1982). Electron microscopic visualization of the tetrodotoxin-binding protein from *Electrophorus electricus*. *Proc. natn. Acad. Sci. U.S.A.* **79**, 4461–4465.
- FOX, J. M. (1976). Ultra-slow inactivation of the ionic currents through the membrane of myelinated nerve. *Biochim. biophys. Acta.* **426**, 232–244.
- GORDON, A. M. & KAO, L. I. (1978). Disorders of muscle membranes: The periodic paralyses. In *Physiology of Membrane Disorders*, chap. 39, ed. ANDREOLI, T. E., HOFFMAN, J. F. & FANESTIL, D. D., pp. 817–829. New York: Plenum Publishing Corp.
- HILLE, B. & CAMPBELL, D. T. (1976). An improved vaseline gap voltage clamp for skeletal muscle fibers. *J. gen. Physiol.* **67**, 265–293.
- HODGKIN, A. L. & HUXLEY, A. F. (1952). A quantitative description of membrane current and its application to conduction and excitation in nerve. *J. Physiol.* **117**, 500–544.
- MCLAUGHLIN, S. & POO, M.-M. (1981). The role of electro-osmosis in the electric-field-induced movement of charged macromolecules on the surface of cells. *Biophys. J.* **34**, 85–93.
- NARAHASHI, T. (1964). Restoration of action potential by anodal polarization in lobster giant axons. *J. cell. comp. Physiol.* **64**, 73–96.
- NEUMCKE, B., FOX, J. M., DROUIN, H. & SCHWARZ, W. (1976). Kinetics of the slow variation of peak sodium current in the membrane of myelinated nerve following changes of holding potential or extracellular pH. *Biochim. biophys. Acta* **426**, 245–257.
- ORIDA, N. & POO, M.-M. (1978). Electrophoretic movement and localisation of acetylcholine receptors in the embryonic muscle cell membrane. *Nature, Lond.* **275**, 31–35.
- PEGANOV, E. M., KHODOROV, B. I. & SHISHKOVA, L. D. (1973). Slow sodium inactivation related to external potassium in the membrane of Ranvier's node. The role of external K (In Russian). *Bull. exp. Biol. Med.* **9**, 15–19.
- POO, M.-M. (1981). *In situ* electrophoresis of membrane components. *A. Rev. Biophys. Bioeng.* **10**, 245–276.
- POO, M.-M., POO, W.-J. & LAM, J. W. (1978). Lateral electrophoresis and diffusion of concanavalin A receptors in the membrane of embryonic muscle cell. *J. Cell Biol.* **76**, 483–501.
- RUDY, B. (1978). Slow inactivation of the sodium conductance in squid giant axons. Pronase resistance. *J. Physiol.* **283**, 1–21.
- RUDY, B. (1981). Inactivation in *Myxicola* giant axons responsible for slow and accumulative adaptation phenomena. *J. Physiol.* **312**, 531–549.

- SCHAUF, C. L. PENCEK, T. L., & DAVIS, F. A. (1976). Slow sodium inactivation in *Myxicola* axons. Evidence for a second inactive state. *Biophys. J.* **16**, 771-778
- STÜHMER, W. & ALMERS, W. (1982). Photobleaching through glass micropipettes: Sodium channels without lateral mobility in the sarcolemma of frog skeletal muscle. *Proc. natn. Acad. Sci. U.S.A.* **79**, 946-950.
- TAYLOR, P. (1980). Neuromuscular blocking agents. In *The Pharmacological Basis of Therapeutics*, ed. GILMAN, A. G., GOODMAN, L. S. & GILMAN, A., 6th edn., pp. 220-234. New York: Macmillan Publishing Co.
- ZAGYANSKY, Y. A. & JARD, S. (1979). Does Lectin-receptor complex formation produce zones of restricted mobility within the membrane? *Nature, Lond.* **280**, 591-593.